

Stable dynamic states at the nematic liquid crystals in weak shear flow

Hui Zhang^{a,*}, Pingwen Zhang^b

^a School of Mathematical Sciences, Beijing Normal University, Beijing, 100875, PR China

^b LMAM and School of Mathematical Sciences, Peking University, Beijing, 100871, PR China

Received 15 November 2006; received in revised form 24 May 2007; accepted 19 June 2007
Available online 26 June 2007

Communicated by M. Vergassola

Abstract

We study stable equilibria of liquid crystals in the flow being at rest and the stable dynamic states for nematic liquid crystals under weak shear flow for the Doi model [M. Doi, S.F. Edwards, *The Theory of Polymer Dynamics*, Oxford University Press, 1986]. It is first theoretically proven that there is a hysteresis phenomenon in the flow being at rest when the non-dimensional potential intensity among particles changes. Furthermore, in the weak shear flow, we show that there exist many stable dynamic states: flow aligning, tumbling, log-rolling and kayaking, which depend on the initial concentrated orientation of liquid crystal particles. The results are consistent with those of numerical simulation [M.G. Forest, Q. Wang, R. Zhou, *The weak shear kinetic phase diagram for nematic polymers*, *Rheol. Acta* 43 (2004) 17–37; M.G. Forest, R. Zhou, Q. Wang, *Full-tensor alignment criteria for sheared nematic polymers*, *J. Rheol.* 47 (2003) 105–127] and experimental discoveries [W.R. Burghardt, *Molecular orientation and rheology in sheared lyotropic liquid crystalline polymers*, *Macromol. Chem. Phys.* 199 (1998) 471–488; Ch. Gähwiller, *Temperature dependence of flow alignment in nematic liquid crystals*, *Phys. Rev. Lett.* 28 (1972) 1554–1556]. Theoretical analysis is reported the first time that the Kayaking state does not circulate around a fixed direction but the asymmetric axis will periodically change.

© 2007 Elsevier B.V. All rights reserved.

Keywords: Nematic liquid crystals; Hysteresis phenomenon; Stable dynamic states; Theoretical analysis

1. Introduction

Four decades of the theoretical and numerical study of homogeneous responses of nematic polymers and liquid crystals to shear flow have led to a fundamental understanding of macromolecular fluids [1,4,5,9,10,18,22,26,27]; more complete references can be found in [17]. These studies aspire to reproduce, explain, and predict experimental discoveries of steady and transient modes [2,3,6,19]. By a combination of theory and experiment, many dynamical and transient modes have been catalogued and named primarily on the basis of director response: steady alignment with a primary director either in the shear plane (flow aligning) or along the vorticity axis (log-rolling); in-plane transient oscillatory (wagging) or rotating (tumbling)

director modes; and out-of plane transient director modes (kayaking) [15–17] and the references therein.

One of the most popular models is the Doi kinetic theory describing rigid macromolecules [10]. It is also called the Smoluchowski equation, which includes the rotation and translation of polymeric molecules convected with the flow. It describes the properties of liquid crystalline polymers in a solvent; see, e.g., [10,12,17,18,26,27]. Its basic feature is its ability to describe both the isotropic and nematic phases, e.g., [10,18,28]. One of the simplest models is

$$\frac{\partial f}{\partial t} = \frac{1}{De} \mathcal{R} \cdot (\mathcal{R}f + f\mathcal{R}U) - \mathcal{R} \cdot (x \times \kappa \cdot xf), \quad (1.1)$$

where $f(t, x)$ denotes the orientation distribution function, and De is the Deborah number, and x denotes the orientation of a rigid-rodlike liquid crystal particle in solvent. Now it is assumed that the lengths of the rods are similar. Therefore, one can suppose that $x \in \mathbb{S}^2$, where \mathbb{S}^2 is the unit sphere,

* Corresponding author. Tel.: +86 10 8514 6281; fax: +86 10 5880 8202.

E-mail addresses: hzhang@bnu.edu.cn (H. Zhang), pzhang@pku.edu.cn (P. Zhang).

$\mathcal{R} = x \times \frac{\partial}{\partial x}$ is an operator, and $\kappa = \nabla v$ with v being the velocity of the flow. From Eq. (1.1) we see that $\int_{|x|=1} f(t, x) dx$ is conserved for any time t . Therefore (1.1) is often solved together with an enforced normalization $\int_{|x|=1} f(t, x) dx = 1$. $U([f])$ is the mean-field interaction potential. Two of the most popular forms are the Onsager form [10,18,28]:

$$U([f]) = \alpha \int_{|x'|=1} |x \times x'| f(x', t) dx'; \quad (1.2)$$

and the Maier–Saupe potential [10,18]

$$U([f]) = \alpha \int_{|x'|=1} |x \times x'|^2 f(x', t) dx', \quad (1.3)$$

where the parameter α measures the potential intensity. In the following discussion one can see that this non-dimensional parameter will play an important role.

The Smoluchowski equation (1.1) is known to exhibit nontrivial nonlinear features, e.g. [7,20], and its study has recently attracted great attention, e.g. [12,26,27]. Phase transitions to equilibrium solutions of this equation with $\kappa = 0$ were first described by Onsager in 1949 [28], using a variational approach; but his argument was based on an assumed explicit ansatz for the distribution function

$$f(x) = \frac{\beta}{4\pi \sinh \beta} \cosh(\beta x \cdot y), \quad (1.4)$$

with the Onsager potential, where $y \in \mathbb{S}^2$ and β is a parameter to be determined from the condition that the free energy be minimized. Using this ansatz Onsager was able to argue that in the limit of high concentration one has a transition from the isotropic uniform distribution to an ordered prolate distribution [28]. The parameter in (1.4) $\beta \sim \alpha$ represents the degree of ordering: $\beta = 0$ corresponds to the isotropic state, and $\beta = \infty$ the completely ordered state. Recently, this transition to order at high concentration was rigorously proved by Constantin et al. [7], where some nice properties of equilibrium solutions were also studied. For the Smoluchowski equation (1.1) restricted on a circle, it has been well understood because of recent efforts [8,9,13,24,25]. For the Smoluchowski equation (1.1) on a sphere, the authors in [14] gave the axial-symmetric property of equilibrium solutions, and critical intensities of phase transitions are observed based on numerical calculation. In [24] we gave not only the axial-symmetric property of equilibrium solutions but also the explicit formulas for all equilibrium solutions and critical intensities of phase transitions for the time-independent Smoluchowski equation $\mathcal{R} \cdot (\mathcal{R}f + f\mathcal{R}U) = 0$ with (2.2). Later these results were proved in [29] by using another approach. However, not all equilibrium solutions are stable. The stability analysis of these solutions is desirable and is one of our goals in this paper. By rigorous analysis it is shown that the stable stationary state of the liquid crystal particles is from the isotropic state to the prolate state when the non-dimensional potential intensity α crosses the critical point 7.5 from small to large, and from the prolate state to the isotropic state when α crosses the other critical point 6.731393 from large to small when the flow is at rest.

With the explicit formulas for all stable equilibria in the flow at rest, we will pay attention to the stable dynamic states at the nematic liquid crystals in the weak shear flow. By perturbation analysis we will show that there are many stable dynamic states in the weak shear flow: (a) steady alignment in the shear-flow aligning and tumbling, (b) along the vorticity axis-log-rolling, (c) out-of plane transient director mode-kayaking. These results are consistent with the responses of numerical simulation [16, 17,22] and experimental discovery [6,19]. Moreover, one can deeply understand the kayaking state, in which rodlike liquid crystal particles do not circulate around a fixed direction but the asymmetric axis will also periodically change. These results basically depend on the explicit expression (3.12) of the critical parameter λ in [21]. Furthermore it is based on the explicit formula of the equilibrium to the rodlike liquid crystal particles at rest flow in [24].

This paper is organized as follows: Section 2 is devoted to the analysis of the stability of the equilibrium states at rest flow. In Section 3 we give the stable dynamic states at the nematic liquid crystals in the weak shear flow. The conclusions are drawn in the final section.

2. Stability of the equilibrium states at rest flow

In this section we will study the stability of the equilibrium solutions, which were obtained in the work [24], for the Eq. (1.1) with $\kappa = 0$, i.e.

$$\mathcal{R} \cdot (\mathcal{R}f + f\mathcal{R}U) = 0 \quad (2.1)$$

with the Maier–Saupe potential [10,18]:

$$U([f]) = \alpha \int_{|x'|=1} |x \times x'|^2 f(x') dx' \quad (2.2)$$

and the normalization

$$\int_{|x|=1} f(x) dx = 1. \quad (2.3)$$

Here we will employ the calculation of a free energy

$$A(f) = \int_{|x|=1} \left[f(x) \ln f(x) + \frac{1}{2} f(x) U([f]) \right] dx \quad (2.4)$$

to analyze the stability of the equilibrium solutions. For self-containment, we first review some important results in [24], where rigorous proofs can also be found. The first result in [24] is about the axial symmetry and explicit representations of the thermodynamic potential U of (2.2).

Lemma 2.1. *Consider the Smoluchowski equation (2.1) with the normalization (2.3). Let U be the thermodynamic potential defined by (2.2). Then such a potential is necessarily invariant with respect to rotations around a director $y \in \mathbb{S}^2$, i.e., it is axially symmetric. Moreover, this potential must have the form*

$$U = \frac{2\alpha}{3} - \eta \left(|x \times y|^2 - \frac{2}{3} \right), \quad (2.5)$$

where $\eta \in \mathbb{R}$ is a parameter.

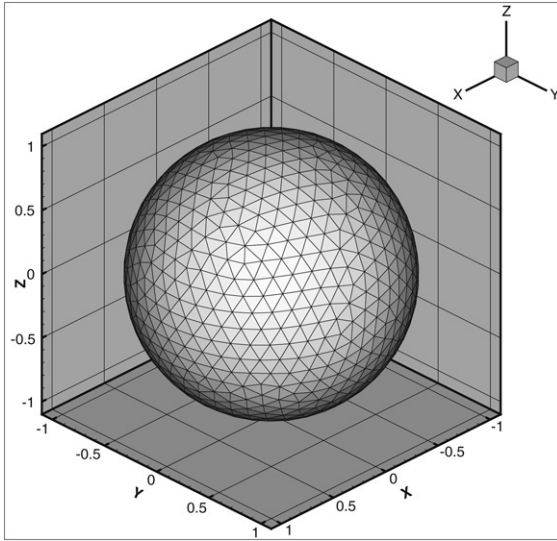


Fig. 1. $\eta = 0$.

The second result in [24] is on the critical intensities of phase transitions and all explicit equilibrium distributions of (2.1).

Lemma 2.2. *The number of equilibrium solutions of the three-dimensional Smoluchowski equation (2.1) with (2.2) and (2.3) hinges on whether the intensity α crosses two critical values: $\alpha^* = 6.731393$ and 7.5. All solutions are given explicitly by*

$$f = ke^{-\eta(x \cdot y)^2}, \tag{2.6}$$

where $y \in \mathbb{S}^2$ is a parameter, $\eta = \eta(\alpha)$ and $k = [4\pi \int_0^1 e^{-\eta z^2} dz]^{-1}$ are determined by α through

$$\frac{e^{-\eta}}{\int_0^1 e^{-\eta z^2} dz} - \left(1 - \frac{2\eta}{3} + \frac{4\eta^2}{3\alpha}\right) = 0. \tag{2.7}$$

More precisely,

- (i) If $0 < \alpha < \alpha^*$, there exists one solution $f_0 = 1/4\pi$.
- (ii) If $\alpha = \alpha^*$, there exist two distinct solutions $f_0 = 1/4\pi$ and $f_1 = k_1 e^{-\eta_1^*(x \cdot y)^2}$, $\eta_1^* < 0$.
- (iii) If $\alpha^* < \alpha < 7.5$, there exist three distinct solutions $f_0 = 1/4\pi$ and $f_i = k_i e^{-\eta_i^*(x \cdot y)^2}$, $\eta_1^* < \eta_2^* < 0$ ($i = 1, 2$).
- (iv) If $\alpha = 7.5$, there exist two distinct solutions $f_0 = 1/4\pi$ and $f_1 = k_1 e^{-\eta_1^*(x \cdot y)^2}$, $\eta_1^* < 0$.
- (v) If $\alpha > 7.5$, there exist three distinct solutions $f_0 = 1/4\pi$ and $f_i = k_i e^{-\eta_i^*(x \cdot y)^2}$ ($i = 1, 2$), $\eta_1^* < 0$, $\eta_2^* > 0$.

In physical terms, an isotropic phase corresponds to the case when the distribution function is $f = 1/4\pi$, and a nematic phase corresponds to the case when f is concentrated at some particular director, which includes the prolate and oblate states. For example, in case (v) of Lemma 2.2, $f_0 = 1/4\pi$ is an isotropic distribution; while the distribution function $f_1 = k_1 e^{-\eta_1^*(x \cdot y)^2}$ ($\eta_1^* < 0$) is concentrated in the direction $\pm y$ (called prolate state) and $f_2 = k_2 e^{-\eta_2^*(x \cdot y)^2}$ ($\eta_2^* > 0$) is concentrated on the equator perpendicular to $\pm y$ (called oblate state). The profiles of these three kinds of equilibrium solutions of (2.6) are shown in Figs. 1–3, where we choose $y = (0, 0, 1)$.

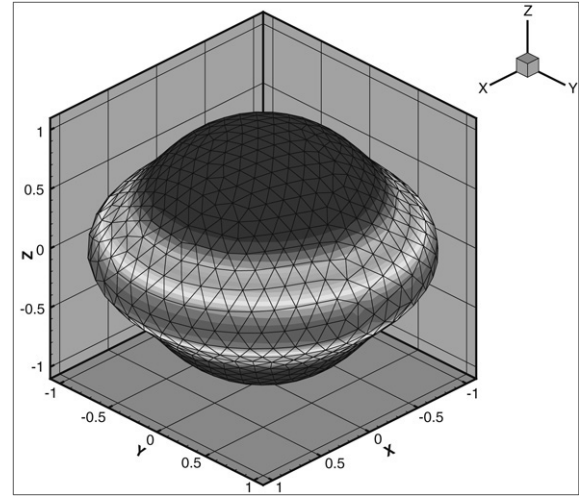


Fig. 2. $\eta = 10$.

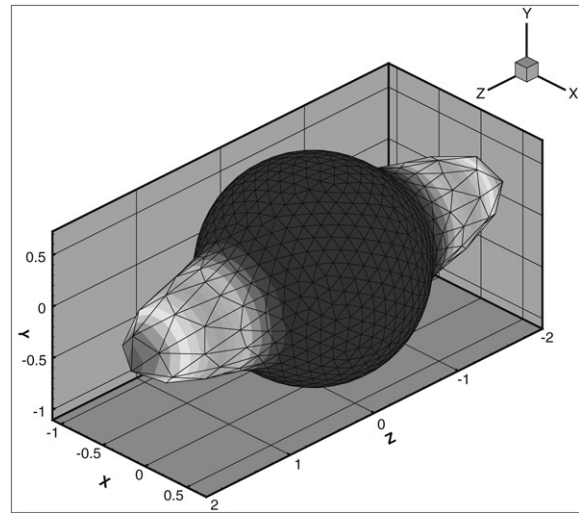


Fig. 3. $\eta = -10$.

Now we state the stability result for the above solutions.

Theorem 2.1. *The stability of the equilibrium solutions to (2.1) with (2.2) and (2.3) obtained in Lemma 2.3 is as follows:*

- (i) If $\alpha \leq \alpha^*$, the constant solution $f = 1/4\pi$ is stable.
- (ii) If $\alpha^* < \alpha < 7.5$, the constant solution $f = 1/4\pi$ is metastable and the nontrivial solution $f = k_1 e^{-\eta_1^*(x \cdot y)^2}$ (prolate) is stable but $f = k_2 e^{-\eta_2^*(x \cdot y)^2}$ (prolate) is unstable.
- (iii) If $\alpha = 7.5$, the nontrivial solution $f = k_1 e^{-\eta_1^*(x \cdot y)^2}$ (prolate) is stable.
- (iv) If $\alpha > 7.5$, the constant solution $f = 1/4\pi$ is unstable while the nontrivial solution $f = k_1 e^{-\eta_1^*(x \cdot y)^2}$ (prolate) is stable but $f = k_2 e^{-\eta_2^*(x \cdot y)^2}$ (oblate) is unstable.

Here η_i^* ($i = 1, 2$) satisfy (2.7) as in Lemma 2.2.

From this theorem we know that the oblate distribution is an unstable equilibrium. Moreover, from the explicit expression of (2.5) and (2.6) and Fig. 3, the direction y in (2.6) is the

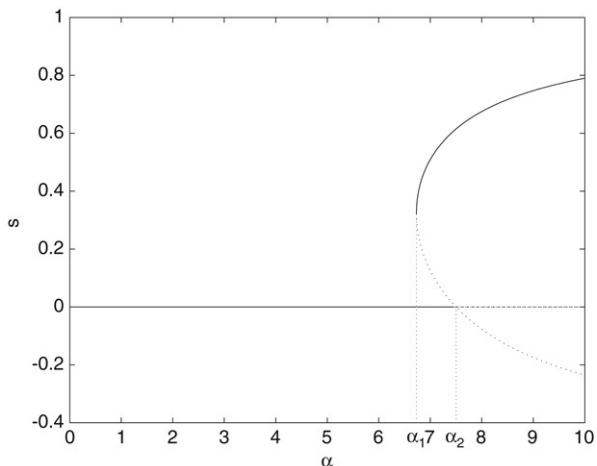


Fig. 4. s vs α : the dashed line is the unstable solution; the solid line is the stable and metastable solution, where $\alpha_1 = \alpha^* = 6.731393$ and $\alpha_2 = 7.5$.

dominated direction of rodlike particles for the stable nematic equilibrium solutions.

Before presenting the proof of Theorem 2.1, we illustrate this equilibrium situation, that is, the stationary solutions at rest for the sake of clarity as [12]. Fig. 4 shows the scalar order parameter s reported versus the nondimensional potential intensity α . The scalar order parameter represents a scalar measure of the degree of the order of the sample. Here

$$s = \frac{3}{2}A, \tag{2.8}$$

where A is the eigenvalue with the largest absolute value of the traceless second-rank order tensor \mathbf{S} given by

$$\mathbf{S} = \langle x \otimes x \rangle - \frac{1}{3}\mathbf{I} = \int_{|x|=1} x \otimes x f(x) dx - \frac{1}{3}\mathbf{I}, \tag{2.9}$$

with \mathbf{I} as the second-rank unit tensor. By using the explicit formula (2.6) of the equilibrium solutions (2.6), we obtain

$$\mathbf{S} = \begin{pmatrix} \frac{\eta}{3\alpha} & & \\ & \frac{\eta}{3\alpha} & \\ & & -\frac{2\eta}{3\alpha} \end{pmatrix}. \tag{2.10}$$

Therefore,

$$s = -\frac{\eta}{\alpha}.$$

The scalar order parameter s is zero when the system is isotropic and the distribution function as in Fig. 1. Conversely, its value is nonzero if some degree of orientation is present. It is positive in the case of prolate distributions (e.g. Fig. 3), and negative for oblate ones (e.g. Fig. 2). In Fig. 4, solid lines represent stable and meta-stable stationary solutions and the dashed lines are unstable stationary solutions. From this figure we can see the hysteresis phenomenon; that is, the stable stationary state is from the isotropic phase to the prolate phase when the potential intensity α crosses the critical point 7.5 from small to large, and from the prolate phase to the isotropic phase

when α crosses the other critical point 6.731393 from large to small.

Proof of Theorem 2.1. Now we rewrite the potential of (2.5) in Lemma 2.1 in the form

$$\begin{aligned} \bar{U} &= \frac{2\alpha}{3} + \zeta(x_1^2 - x_2^2) + \eta \left(x_3^2 - \frac{1}{3} \right) \\ &= \frac{2\alpha}{3} + \zeta \sin^2 \theta \cos 2\varphi + \eta \left(\cos^2 \theta - \frac{1}{3} \right). \end{aligned}$$

Then the solution of (2.1) with (2.2) and (2.3) is

$$f = k e^{-\bar{U}} = \frac{e^{-g(z,\varphi)}}{\int_0^{2\pi} \int_0^1 e^{-g(z,\varphi)} dz d\varphi}, \tag{2.11}$$

where $k = \int_{|x|=1} e^{-\bar{U}} dx$, $g(z, \varphi) = \zeta(1 - z^2) \cos 2\varphi + \eta z^2$. Thus the corresponding free energy with (2.11) is a function of ζ, η for fixed $\alpha > 0$ and can be expressed by

$$\begin{aligned} A_\alpha(\zeta, \eta) &= \int_{|x|=1} \left[f(x) \ln f(x) + \frac{1}{2} f(x) U(x) \right] dx \\ &= -\ln 2 \int_0^{2\pi} \int_0^1 e^{-g(z,\varphi)} dz d\varphi - \eta \langle z^2 \rangle_* \\ &\quad - \zeta \langle (1 - z^2) \cos 2\varphi \rangle_* + \frac{\alpha}{2} [1 - (q_1^2 + q_2^2 + q_3^2)], \end{aligned} \tag{2.12}$$

where

$$\langle h(z, \varphi) \rangle_* = \frac{\int_0^{2\pi} \int_0^1 h(z, \varphi) e^{-g(z,\varphi)} dz d\varphi}{\int_0^{2\pi} \int_0^1 e^{-g(z,\varphi)} dz d\varphi} \tag{2.13}$$

$$q_1 = \langle (1 - z^2) \cos^2 \varphi \rangle_*, \tag{2.14}$$

$$q_2 = \langle (1 - z^2) \sin^2 \varphi \rangle_*, \tag{2.15}$$

$$q_3 = \langle z^2 \rangle_*. \tag{2.16}$$

Next, for ease of notation we denote $\langle h(z, \varphi) \rangle = \langle h(z, \varphi) \rangle_*|_{\zeta=0}$. Firstly, we give the following properties of the free energy $A_\alpha(\zeta, \eta^*)$ for η^* satisfying (2.7).

Lemma 2.3. For the η^* satisfying (2.7), the free energy $A_\alpha(\zeta, \eta^*)$ possesses the following properties:

$$\frac{\partial}{\partial \zeta} A_\alpha(0, \eta^*) = 0, \quad \frac{\partial}{\partial \eta} A_\alpha(0, \eta^*) = 0, \quad \eta^* = 0, \eta_1^*, \eta_2^*,$$

$$\frac{\partial^2}{\partial \eta \partial \zeta} A_\alpha(0, \eta) = 0.$$

Moreover:

- (i) If $\alpha < \alpha^*$, $\frac{\partial^2}{\partial \zeta^2} A_\alpha(0, 0) > 0$, $\frac{\partial^2}{\partial \eta^2} A_\alpha(0, 0) > 0$.
- (ii) If $\alpha = \alpha^*$, then

$$\begin{aligned} \frac{\partial^2}{\partial \zeta^2} A_\alpha(0, 0) &> 0, & \frac{\partial^2}{\partial \eta^2} A_\alpha(0, 0) &> 0; \\ \frac{\partial^2}{\partial \zeta^2} A_\alpha(0, \eta_1^*) &> 0, & \frac{\partial^2}{\partial \eta^2} A_\alpha(0, \eta_1^*) &= 0. \end{aligned}$$

(iii) If $\alpha^* < \alpha < 7.5$, then

$$\begin{aligned} \frac{\partial^2}{\partial \zeta^2} A_\alpha(0, 0) &> 0, & \frac{\partial^2}{\partial \eta^2} A_\alpha(0, 0) &> 0; \\ \frac{\partial^2}{\partial \zeta^2} A_\alpha(0, \eta_1^*) &> 0, & \frac{\partial^2}{\partial \eta^2} A_\alpha(0, \eta_1^*) &> 0; \\ \frac{\partial^2}{\partial \zeta^2} A_\alpha(0, \eta_2^*) &> 0, & \frac{\partial^2}{\partial \eta^2} A_\alpha(0, \eta_2^*) &< 0. \end{aligned}$$

(iv) If $\alpha = 7.5$, then

$$\begin{aligned} \frac{\partial^2}{\partial \zeta^2} A_\alpha(0, 0) &> 0, & \frac{\partial^2}{\partial \eta^2} A_\alpha(0, 0) &= 0; \\ \frac{\partial^2}{\partial \zeta^2} A_\alpha(0, \eta_1^*) &> 0, & \frac{\partial^2}{\partial \eta^2} A_\alpha(0, \eta_1^*) &> 0. \end{aligned}$$

(v) If $\alpha > 7.5$, then

$$\begin{aligned} \frac{\partial^2}{\partial \zeta^2} A_\alpha(0, 0) &> 0, & \frac{\partial^2}{\partial \eta^2} A_\alpha(0, 0) &< 0; \\ \frac{\partial^2}{\partial \zeta^2} A_\alpha(0, \eta_1^*) &> 0, & \frac{\partial^2}{\partial \eta^2} A_\alpha(0, \eta_1^*) &> 0; \\ \frac{\partial^2}{\partial \zeta^2} A_\alpha(0, \eta_2^*) &< 0, & \frac{\partial^2}{\partial \eta^2} A_\alpha(0, \eta_2^*) &> 0. \end{aligned}$$

Here η_i^* ($i = 1, 2$) are as in Lemma 2.2.

Under the property of the free energy $A_\alpha(\zeta, \eta^*)$ for η^* satisfying (2.7), we can easily obtain the result of Theorem 2.1. For example, from Lemma 2.3 we know that $(0, \eta_1^*)$ is a minimum point of $A_\alpha(\zeta, \eta)$, while $(0, 0)$ and $(0, \eta_2^*)$ are saddle points of $A_\alpha(\zeta, \eta)$ when $\alpha > 7.5$. Therefore, the solution $f = k_1 e^{-\eta_1^*(x \cdot y)^2}$ is stable, while the solutions $f = 1/4\pi$ and $f = k_2 e^{-\eta_2^*(x \cdot y)^2}$ are unstable. This is (iv) of Theorem 2.1. The other cases are proved in a similar way. \square

Proof of Lemma 2.3. From the formula (2.12), we can verify that

$$\begin{aligned} &\frac{\partial}{\partial \zeta} A_\alpha(0, \eta) \\ &= \left[\eta \left\langle z^2 \frac{\partial g}{\partial \zeta} \right\rangle_* - \eta \langle z^2 \rangle_* \left\langle \frac{\partial g}{\partial \zeta} \right\rangle_* - \alpha \left(\sum_{i=1}^3 q_i \frac{\partial q_i}{\partial \zeta} \right) \right]_{\zeta=0} \\ &= 0, \quad \text{for all } \eta, \end{aligned} \tag{2.17}$$

where we used

$$q_1|_{\zeta=0} = q_2|_{\zeta=0} = \frac{1}{2} \langle 1 - z^2 \rangle, \quad q_3|_{\zeta=0} = \langle z^2 \rangle, \tag{2.18}$$

$$\begin{aligned} \frac{\partial q_1}{\partial \zeta} \Big|_{\zeta=0} &= -\frac{1}{4} \langle (1 - z^2)^2 \rangle, \\ \frac{\partial q_2}{\partial \zeta} \Big|_{\zeta=0} &= \frac{1}{4} \langle (1 - z^2)^2 \rangle, \quad \frac{\partial q_3}{\partial \zeta} \Big|_{\zeta=0} = 0. \end{aligned} \tag{2.19}$$

Further, we can verify

$$\frac{\partial^2}{\partial \zeta^2} A_\alpha(0, \eta) = \left[-\eta \left\langle z^2 \left(\frac{\partial g}{\partial \zeta} \right)^2 \right\rangle_* \right.$$

$$\begin{aligned} &+ \eta \langle z^2 \rangle_* \left\langle \left(\frac{\partial g}{\partial \zeta} \right)^2 \right\rangle_* + \left\langle \left(\frac{\partial g}{\partial \zeta} \right)^2 \right\rangle_* \\ &+ \alpha \left(\sum_{i=1}^3 \left[q_i \frac{\partial^2 q_i}{\partial \zeta^2} + \left(\frac{\partial q_i}{\partial \zeta} \right)^2 \right] \right) \Big|_{\zeta=0} \tag{2.20} \\ &= \frac{1}{2} \langle (1 - z^2)^2 \rangle - \frac{\alpha}{8} \langle (1 - z^2)^2 \rangle^2 - \frac{\eta}{2} \langle z^2 (1 - z^2)^2 \rangle \\ &+ \frac{\eta}{2} \langle z^2 \rangle \langle (1 - z^2)^2 \rangle \\ &- \alpha \left[\frac{\langle 1 - z^2 \rangle}{4} (\langle (1 - z^2)^3 \rangle - \langle 1 - z^2 \rangle \langle (1 - z^2)^2 \rangle) \right] \\ &- \alpha \left[\frac{\langle z^2 \rangle}{2} (\langle z^2 (1 - z^2)^2 \rangle - \langle z^2 \rangle \langle (1 - z^2)^2 \rangle) \right], \end{aligned} \tag{2.21}$$

where we used

$$\begin{aligned} \frac{\partial^2 q_1}{\partial \zeta^2} \Big|_{\zeta=0} &= \frac{\partial^2 q_2}{\partial \zeta^2} \Big|_{\zeta=0} \\ &= \frac{1}{4} \langle (1 - z^2)^3 \rangle - \frac{1}{4} \langle 1 - z^2 \rangle \langle (1 - z^2)^2 \rangle, \\ \frac{\partial^2 q_3}{\partial \zeta^2} \Big|_{\zeta=0} &= \frac{1}{2} \langle z^2 (1 - z^2)^2 \rangle - \frac{1}{2} \langle z^2 \rangle \langle (1 - z^2)^2 \rangle. \end{aligned}$$

From [24], we know that α and η satisfy $\langle z^2 \rangle = \frac{1}{3} - \frac{2\eta}{3\alpha}$. Then inserting

$$\eta = \frac{\alpha}{2} (1 - 3\langle z^2 \rangle) \tag{2.22}$$

into (2.20), the last terms of (2.20) can be written as

$$\begin{aligned} &-\frac{\eta}{2} \langle z^2 (1 - z^2)^2 \rangle + \frac{\eta}{2} \langle z^2 \rangle \langle (1 - z^2)^2 \rangle \\ &- \alpha \left[\frac{\langle 1 - z^2 \rangle}{4} (\langle (1 - z^2)^3 \rangle - \langle 1 - z^2 \rangle \langle (1 - z^2)^2 \rangle) \right] \\ &- \alpha \left[\frac{\langle z^2 \rangle}{2} (\langle z^2 (1 - z^2)^2 \rangle - \langle z^2 \rangle \langle (1 - z^2)^2 \rangle) \right] \\ &= \alpha \frac{1 - \langle z^2 \rangle}{4} [\langle (1 - z^2)^2 \rangle - \langle z^2 (1 - z^2)^2 \rangle - \langle (1 - z^2)^3 \rangle] \\ &= 0. \end{aligned}$$

Therefore, for (2.20), we have

$$\begin{aligned} \frac{\partial^2}{\partial \zeta^2} A_\alpha(0, \eta) &= \frac{1}{2} \langle (1 - z^2)^2 \rangle - \frac{\alpha}{8} \langle (1 - z^2)^2 \rangle^2 \\ &= \frac{1}{2} \langle (1 - z^2)^2 \rangle \left(1 - \frac{\alpha}{4} \langle (1 - z^2)^2 \rangle \right) \\ &= \frac{1}{12} \langle (1 - z^2)^2 \rangle \left(\frac{15}{2} - \alpha - \eta \right), \end{aligned} \tag{2.23}$$

where we used

$$\langle z^2 \rangle - \langle z^4 \rangle = \frac{1}{\alpha}, \tag{2.24}$$

from [24]. By (2.23), we can thus derive the corresponding properties in Lemma 2.3 for $\eta^* = 0, \eta_1^*, \eta_2^*$.

From (2.12) we have

$$\begin{aligned} \frac{\partial}{\partial \eta} A_\alpha(0, \eta) &= -\eta(\langle z^2 \rangle^2 - \langle z^4 \rangle) - \alpha \left(\sum_{i=1}^3 q_i \frac{\partial q_i}{\partial \eta} \right) \Big|_{\zeta=0} \\ &= 0, \end{aligned} \quad (2.25)$$

for η satisfying (2.7) in the formula (2.6) of the equilibrium solution. Here we used (2.22) and (2.18) and

$$\begin{aligned} \frac{\partial q_1}{\partial \eta} \Big|_{\zeta=0} &= \frac{\partial q_2}{\partial \eta} \Big|_{\zeta=0} = \frac{1}{2}(\langle z^4 \rangle - \langle z^2 \rangle^2), \\ \frac{\partial q_3}{\partial \eta} \Big|_{\zeta=0} &= -\langle z^4 \rangle + \langle z^2 \rangle^2. \end{aligned}$$

This shows that the η^* satisfying (2.7) is the extreme point of $A_\alpha(0, \eta)$. Further, using the relations

$$\begin{aligned} \frac{\partial^2 q_1}{\partial \eta^2} \Big|_{\zeta=0} &= \frac{\partial^2 q_2}{\partial \eta^2} \Big|_{\zeta=0} = -\frac{1}{2}[\langle z^6 \rangle - 3\langle z^2 \rangle \langle z^4 \rangle + 2\langle z^2 \rangle^3] \\ \frac{\partial^2 q_3}{\partial \eta^2} \Big|_{\zeta=0} &= \langle z^6 \rangle - 3\langle z^2 \rangle \langle z^4 \rangle + 2\langle z^2 \rangle^3, \end{aligned}$$

we have

$$\begin{aligned} \frac{\partial^2}{\partial \eta^2} A_\alpha(0, \eta) &= \langle z^4 \rangle - \langle z^2 \rangle^2 - \eta[\langle z^6 \rangle - 3\langle z^2 \rangle \langle z^4 \rangle + 2\langle z^2 \rangle^3] \\ &\quad - \alpha \left(\frac{1}{2}(\langle z^2 \rangle - 1)[\langle z^6 \rangle - 3\langle z^2 \rangle \langle z^4 \rangle \right. \\ &\quad \left. + 2\langle z^2 \rangle^3] + \frac{3}{2}(\langle z^4 \rangle - \langle z^2 \rangle^2) \right) \\ &= (\langle z^4 \rangle - \langle z^2 \rangle^2) \left(1 - \frac{3\alpha}{2}(\langle z^4 \rangle - \langle z^2 \rangle^2) \right) \\ &= \frac{1}{6\alpha}(\langle z^4 \rangle - \langle z^2 \rangle^2)(15\alpha - 2\alpha^2 + 2\alpha\eta + 4\eta^2), \end{aligned} \quad (2.26)$$

where we used (2.23) and (2.24). For η^* satisfying (2.7), we see that the sign of $\frac{\partial^2}{\partial \eta^2} A_\alpha(0, \eta^*)$ is determined by

$$Q \triangleq 4\eta^{*2} + 2\alpha\eta^* + 15\alpha - 2\alpha^2. \quad (2.27)$$

When $\alpha > 20/3$, (2.27) can also be rewritten as

$$Q = (\eta^* - \bar{\eta}_1)(\eta^* - \bar{\eta}_2), \quad (2.28)$$

where

$$\begin{aligned} \bar{\eta}_1 &= -\frac{\alpha}{4} \left(1 + 3\sqrt{1 - \frac{20}{3\alpha}} \right), \\ \bar{\eta}_2 &= -\frac{\alpha}{4} \left(1 - 3\sqrt{1 - \frac{20}{3\alpha}} \right). \end{aligned} \quad (2.29)$$

From the argument in [24] we know that $\eta_1^* < \bar{\eta}_1$ and $\bar{\eta}_1 < \eta_2^* < \bar{\eta}_2 < 0$ if $20/3 < \alpha < 7.5$, but $\eta_2^* > \bar{\eta}_2 > 0$ if $\alpha > 7.5$. Thus we can obtain that $\frac{\partial^2}{\partial \eta^2} A_\alpha(0, \eta_1^*) > 0$, and $\frac{\partial^2}{\partial \eta^2} A_\alpha(0, \eta_2^*) < 0$ if $\alpha^* < \alpha < 7.5$. While $\frac{\partial^2}{\partial \eta^2} A_\alpha(0, \eta_1^*) > 0$ and $\frac{\partial^2}{\partial \eta^2} A_\alpha(0, \eta_2^*) > 0$ if $\alpha > 7.5$. (2.27) yield $\frac{\partial^2}{\partial \eta^2} A_\alpha(0, 0) < 0$

if $\alpha > 15/2$, and $\frac{\partial^2}{\partial \eta^2} A_\alpha(0, 0) > 0$ if $\alpha < 15/2$. The proof of Lemma 2.3 is now complete. \square

3. Stable dynamic states in the weak shear flow

It is well known that the constitutive equation for the nematic liquid crystals under weak velocity gradient is derived from the kinetic equation, as presented by Doi [21]. The constitutive equation is consistent with the phenomenological equation proposed by Ericksen and Leslie. The six viscosity parameters (Leslie coefficients) appearing in the phenomenological theory are expressed by the molecular parameters. Recently the authors in [11] have completed the model for the inhomogeneous kinetic theory of rodlike LCPs and showed that the inhomogeneous theory properly reduces to the Ericksen–Leslie theory in the limit of the small Deborah number. Furthermore, there are papers [15–17,22,23] on the numerical simulation works of these models, and some experiments [3,19] to discover the dynamic states in the weak shear flow. However, there do not seem to exist theoretical results on the stable dynamic states for nematic liquid crystals under weak velocity gradient. This is our aim in this section.

We now choose the solution of (1.1) in the form of a perturbation series,

$$f = f_0 + De f_1 + \dots \quad (3.1)$$

where f_0 denotes the equilibrium distribution function and f_1 is the first-order perturbation. And setting $U(x, [f_1]) = \alpha \int_{|x|=1} |x \times x'|^2 f_1(x') dx'$, we have

$$\begin{aligned} U(x, [f]) &= U(x, [f_0]) + De U(x, [f_1]) \\ &\quad + \dots \triangleq U_0 + De U_1 + \dots \end{aligned} \quad (3.2)$$

Substituting (3.1) and (3.2) into (1.1), we obtain the equations for f_0 and f_1 respectively to order De^{-1} and De^0 ,

$$De^{-1} : \mathcal{R} \cdot \mathcal{R} f_0 + \mathcal{R} \cdot (f_0 \mathcal{R} U_0) = 0, \quad (3.3)$$

$$De^0 : -F f_1 = \frac{df_0}{dt} - \mathcal{R} \cdot (x \times \kappa \cdot x f_0), \quad (3.4)$$

where the operator F is given by

$$F \phi = -\mathcal{R} \cdot (\mathcal{R} \phi + \phi \mathcal{R} U_0 + f_0 \mathcal{R} U(x, [\phi])). \quad (3.5)$$

For the equation to order De^1 , we can see that there is a term $\frac{df_1}{dt}$; but we consider the Deborah number De to be very small. Therefore, here we omit the higher-order equations. Moreover we remark that the perturbation series (3.1) depends on the Deborah number. While there is another perturbation method in [30] depending not only on the Deborah number but also on a slow scale time introduced by Zhou and Wang, the result obtained is partially similar.

Now set ψ_0 to be the eigenfunction of the Hermitian conjugate operator F^* of F corresponding to the zero eigenvalue, i.e.

$$F^* \psi_0 = 0. \quad (3.6)$$

Kuzuu and Doi [21] found a solution in the form

$$\psi_0(x) = \Theta \cdot e_{\varphi g}(\theta), \quad (3.7)$$

where Θ is an arbitrary constant vector, e_φ is the unit vector for the spherical coordinate φ , and g satisfies

$$\begin{aligned} & \frac{1}{\sin \theta} \frac{d}{d\theta} \left(\sin \theta \frac{dg}{d\theta} \right) - \frac{g}{\sin^2 \theta} - \frac{dU([f_0])}{d\theta} \frac{dg}{d\theta} \\ &= -\frac{dU([f_0])}{d\theta}. \end{aligned} \quad (3.8)$$

Similarly to the argument in [11,21], since we consider only the weak shear flow, we assume that the main term f_0 in (3.1) determines the dominated direction of rodlike particles for the nematic equilibrium solutions, denoted by $\mathbf{n}(t)$. From (3.4), taking the inner product with the eigenfunction ψ_0 of the operator F^* with zero eigenvalue, one obtains:

$$\begin{aligned} \int_{|x|=1} \psi_0 \frac{df_0}{dt} dx &= \int_{|x|=1} \psi_0 f_0' (x \cdot \mathbf{n}(t)) x \cdot \dot{\mathbf{n}} dx \\ &= \dot{\mathbf{n}} \times \mathbf{n} \cdot \int_{|x|=1} \psi_0 \mathcal{R} f_0 dx \\ &= \mathbf{n} \times \dot{\mathbf{n}} \cdot \langle \mathcal{R} \psi_0 \rangle = \Theta \cdot (\mathbf{n} \times \dot{\mathbf{n}}) \frac{s}{\lambda}, \end{aligned}$$

and

$$\begin{aligned} & \int_{|x|=1} \psi_0 \mathcal{R} \cdot (x \times \kappa \cdot x f_0) dx \\ &= - \int_{|x|=1} \mathcal{R} \psi_0 \cdot (x \times \kappa \cdot x f_0) dx \\ &= \kappa : \langle x \otimes x \times \mathcal{R} \psi_0 \rangle \\ &= \Theta \cdot \mathbf{n} \times \left(s \mathbf{D} \cdot \mathbf{n} - \frac{s}{\lambda} \Omega \cdot \mathbf{n} \right), \end{aligned}$$

where $\Omega = (\kappa^T - \kappa)/2$, $\mathbf{D} = (\kappa^T + \kappa)/2$, $s = \frac{1}{2}(3\langle \cos^2 \theta \rangle - 1)$ is the order parameter, and

$$\lambda = \frac{2s}{\langle g \frac{dU([f_0])}{d\theta} \rangle}. \quad (3.9)$$

We will see from (3.4) that the evolution of the time-dependent and distortional terms reduces to an equation governing the rotation of the direct \mathbf{n} . In terms of the rotation relative to the background fluid: $\mathbf{N} = \dot{\mathbf{n}} + \Omega \cdot \mathbf{n}$, this equation can be written as

$$\mathbf{n} \times \left(\frac{s}{\lambda} \mathbf{N} - s \mathbf{D} \cdot \mathbf{n} \right) = 0. \quad (3.10)$$

Here we explain that the reduction of (3.10) is physically reasonable since we consider the Deborah number $De \ll 1$ and we assume f_1 is bounded. Therefore, the main leading term in (3.1) is f_0 . Thus, we have to determine that f_0 (3.10) is dependent on f_0 .

Using the explicit expression Eq. (2.6) of f_0 we can now calculate

$$\begin{aligned} U([f_0]) &= \alpha \int_{|x|=1} |x \times x'|^2 f_0(x') dx' \\ &= \alpha \left[1 - \int_{|x|=1} (x \cdot x')^2 k e^{-\eta(x' \cdot \mathbf{n})^2} dx' \right] \\ &= \alpha \left[1 - \frac{1 - \cos^2 \theta}{2} + k \frac{1 - 3 \cos^2 \theta}{2} \right] \end{aligned}$$

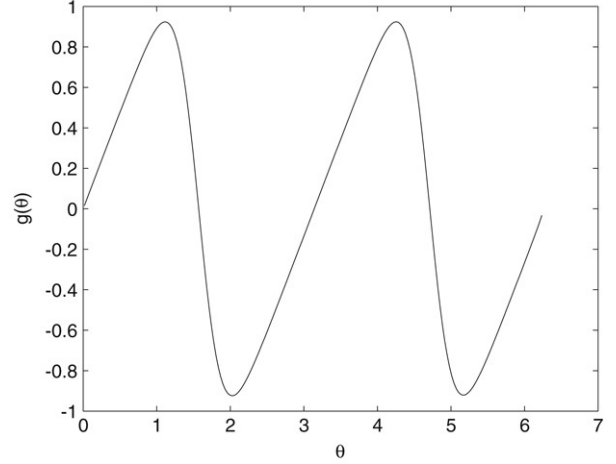


Fig. 5. $g(\theta)$ with $g(0) = g(2\pi)$.

$$\begin{aligned} & \times \int_0^{2\pi} \int_0^\pi \cos^2 \theta' e^{-\eta \cos^2 \theta'} \sin \theta' d\theta' d\varphi \Big] \\ &= \alpha \left[1 - \frac{1 - \cos^2 \theta}{2} + \frac{1 - 3 \cos^2 \theta}{2} 4\pi k \int_0^1 z^2 e^{-\eta z^2} dz \right] \\ &= \alpha \left[1 - \frac{1 - \cos^2 \theta}{2} + \frac{1 - 3 \cos^2 \theta}{2} \left(\frac{1}{3} - \frac{2\eta}{3\alpha} \right) \right] \\ &= \frac{\alpha}{2} \left[1 + \cos^2 \theta + (1 - 3 \cos^2 \theta) \left(\frac{1}{3} - \frac{2\eta}{3\alpha} \right) \right]. \end{aligned}$$

Therefore,

$$\frac{dU([f_0])}{d\theta} = -2\eta \cos \theta \sin \theta.$$

Thus, Eq. (3.8) can be rewritten as

$$\begin{aligned} \sin \theta \frac{d}{d\theta} \left(\sin \theta \frac{dg}{d\theta} \right) - g + \eta \sin^2 \theta \sin 2\theta \frac{dg}{d\theta} \\ = \eta \sin 2\theta \sin^2 \theta. \end{aligned} \quad (3.11)$$

With the periodic boundary condition $g(0) = g(2\pi)$, we can simulate the profile of g to as in Fig. 5.

By the calculation in Section 2 we know that $s = -\frac{\eta}{\alpha}$. Thus we can obtain the explicit formula of the parameter λ ,

$$\begin{aligned} \lambda &= \frac{2s}{\langle g \frac{dU([f_0])}{d\theta} \rangle} = -\frac{2\eta}{\alpha} \frac{1}{\langle -g(\theta) 2\eta \cos \theta \sin \theta \rangle} \\ &= \frac{2}{\alpha} \frac{1}{\langle g(\theta) \sin 2\theta \rangle}. \end{aligned} \quad (3.12)$$

By numerical calculation, we plot the relation between λ and α in Fig. 6. We can see that $\lambda > 1$ if $\alpha^* < \alpha < \bar{\alpha}$ and $\lambda < 1$ if $\alpha > \bar{\alpha}$, where $\bar{\alpha} \approx 7.88$. Here we especially point out that Eq. (3.11) of g and the parameter formula (3.12) of λ can be explicitly given since we have the explicit expression (2.6) of f_0 in [24]. But g and λ in [21] are implicit functions depending on f_0 . Hereafter one will see that the explicit formula (3.12) of the parameter λ plays an important role in the analysis of the stable dynamic states of liquid crystal particles in the weak shear flow.

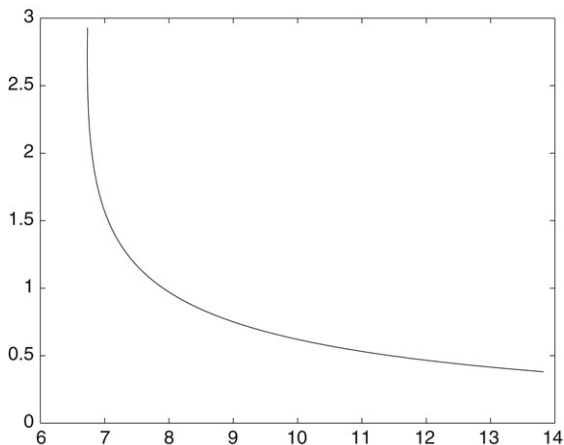


Fig. 6. The relation of λ and α .

We now set $\mathbf{n} = (n_1, n_2, n_3)^T$ and for weak shear flow we denote

$$\kappa = \begin{pmatrix} 0 & 0 & \gamma \\ 0 & 0 & 0 \\ 0 & 0 & 0 \end{pmatrix},$$

where γ is the shear rate. Then (3.10) can be written as

$$\frac{s}{\lambda} \dot{n}_1 - \frac{s\gamma}{2} \left(1 + \frac{1}{\lambda}\right) n_3 = Ln_1, \tag{3.13}$$

$$\frac{s}{\lambda} \dot{n}_2 = Ln_2, \tag{3.14}$$

$$\frac{s}{\lambda} \dot{n}_3 - \frac{s\gamma}{2} \left(1 - \frac{1}{\lambda}\right) n_1 = Ln_3 \tag{3.15}$$

where L is a parameter. (3.13) · n_1 + (3.14) · n_2 + (3.15) · n_3 yields

$$L = -s\gamma n_1 n_3, \tag{3.16}$$

where we used $n_1^2 + n_2^2 + n_3^2 = 1$. Thus the Eqs. (3.13)–(3.15) can be rewritten in the form

$$\dot{n}_1 - \frac{\gamma}{2}(\lambda + 1)n_3 = -\lambda\gamma n_1^2 n_3, \tag{3.17}$$

$$\dot{n}_2 = -\lambda\gamma n_1 n_2 n_3, \tag{3.18}$$

$$\dot{n}_3 - \frac{\gamma}{2}(\lambda - 1)n_1 = -\lambda\gamma n_1 n_3^2. \tag{3.19}$$

If we rescale time,

$$t = \gamma\tau,$$

then the above Eqs. (3.17)–(3.19) become

$$\frac{d}{d\tau} n_1 - \frac{1}{2}(\lambda + 1)n_3 = -\lambda n_1^2 n_3, \tag{3.20}$$

$$\frac{d}{d\tau} n_2 = -\lambda n_1 n_2 n_3, \tag{3.21}$$

$$\frac{d}{d\tau} n_3 - \frac{1}{2}(\lambda - 1)n_1 = -\lambda n_1 n_3^2. \tag{3.22}$$

Let

$$n_2 = \cos \theta, \quad n_1 = \sin \theta \cos \psi, \quad n_3 = \sin \theta \sin \psi. \tag{3.23}$$

Therefore, we obtain the equations of θ, ψ :

$$\frac{d\theta}{d\tau} = \frac{\lambda}{4} \sin 2\theta \sin 2\psi, \tag{3.24}$$

$$\frac{d\psi}{d\tau} = -\frac{1}{2}(1 - \lambda \cos 2\psi). \tag{3.25}$$

Thus, we only need to analyze Eqs. (3.24) and (3.25) in order to know the stable dynamic state of (3.20)–(3.22).

From (3.24) and (3.25), we know that when $\lambda \geq 1$ the equilibrium points of (3.24) and (3.25) satisfy

$$\sin 2\theta = 0, \quad 1 - \lambda \cos 2\psi = 0.$$

Thus, there are these two equilibrium points: $(0, \frac{1}{2} \arccos \frac{1}{\lambda})$ and $(\frac{\pi}{2}, \frac{1}{2} \arccos \frac{1}{\lambda})$. Next, we study the stability of two equilibrium points.

(1) For the equilibrium point $(0, \frac{1}{2} \arccos \frac{1}{\lambda})$, let $\xi = \theta, \eta = \psi - \frac{1}{2} \arccos \frac{1}{\lambda}$. We then obtain

$$\frac{d\xi}{d\tau} = b(\lambda)\xi + a_1(\xi, \eta) \tag{3.26}$$

$$\frac{d\psi}{d\tau} = -2b(\lambda)\eta + a_2(\xi, \eta), \tag{3.27}$$

where $b(\lambda) = \frac{\lambda}{2} \sin \arccos \frac{1}{\lambda}$ and $a_i(\xi, \eta)$ ($i = 1, 2$) are nonlinear terms of ξ, η . This shows that there is a saddle point. Thus $(0, \frac{1}{2} \arccos \frac{1}{\lambda})$ is an unstable equilibrium point.

(2) For the other equilibrium point $(\frac{\pi}{2}, \frac{1}{2} \arccos \frac{1}{\lambda})$, similarly, setting $\xi = \theta - \frac{\pi}{2}, \eta = \psi - \frac{1}{2} \arccos \frac{1}{\lambda}$, we have

$$\frac{d\xi}{d\tau} = -b(\lambda)\xi + a_1(\xi, \eta) \tag{3.28}$$

$$\frac{d\psi}{d\tau} = -2b(\lambda)\eta + a_2(\xi, \eta). \tag{3.29}$$

This implies that $(\frac{\pi}{2}, \frac{1}{2} \arccos \frac{1}{\lambda})$ is an asymptotically stable equilibrium point.

Therefore, from (3.23), the stable equilibrium directors are

$$\begin{aligned} n_2 &= \cos \frac{\pi}{2} = 0, \\ n_1 &= \cos \left(\frac{1}{2} \arccos \frac{1}{\lambda} \right) = \pm \sqrt{\frac{\lambda + 1}{2\lambda}}, \\ n_3 &= \sin \left(\frac{1}{2} \arccos \frac{1}{\lambda} \right) = \pm \sqrt{\frac{\lambda - 1}{2\lambda}}. \end{aligned} \tag{3.30}$$

In the following we study the case $0 < \lambda < 1$. In this case $\frac{d\psi}{d\tau} < 0$, so ψ is a decreasing function of τ . Hence we can set $\psi = a(\tau)$, where $a'(\tau) < 0$. One can find from (3.25) that ψ is uniquely determined by the implicit equation

$$\frac{1}{\sqrt{1 - \lambda^2}} \arctan \frac{\sqrt{1 - \lambda^2} \sin 2\psi}{\lambda - \cos 2\psi} = \tau + C_0, \tag{3.31}$$

with C_0 depending on the initial value of ψ . Thus we have from (3.24),

$$\frac{d\theta}{d\tau} = \frac{\lambda}{4} \sin 2\theta \sin 2a(\tau). \tag{3.32}$$

We can solve it by integrating the formula

$$\frac{1}{\sin 2\theta} d\theta = \frac{\lambda}{4} \sin 2a(\tau) d\tau,$$

from 0 to τ . Thus,

$$\frac{1 - \cos 2\theta}{1 + \cos 2\theta} = C e^{\lambda \int_0^\tau \sin 2a(t) dt},$$

where

$$C = \frac{1 - \cos 2\theta(0)}{1 + \cos 2\theta(0)} \quad (3.33)$$

depends on the initial value of $\theta(\tau)$. We can see that $C \geq 0$. This yields

$$\cos 2\theta = \frac{1 - C e^{\lambda \int_0^\tau \sin 2a(t) dt}}{1 + C e^{\lambda \int_0^\tau \sin 2a(t) dt}}.$$

Therefore, we obtain from (3.23):

$$n_2 = \cos \theta = \pm \sqrt{\frac{1}{1 + C e^{\lambda \int_0^\tau \sin 2a(t) dt}}}, \quad (3.34)$$

$$n_1 = \sin \theta \cos \psi = \pm \sqrt{\frac{C e^{\lambda \int_0^\tau \sin 2a(t) dt}}{1 + C e^{\lambda \int_0^\tau \sin 2a(t) dt}}} \cos a(\tau), \quad (3.35)$$

$$n_3 = \sin \theta \sin \psi = \pm \sqrt{\frac{C e^{\lambda \int_0^\tau \sin 2a(t) dt}}{1 + C e^{\lambda \int_0^\tau \sin 2a(t) dt}}} \sin a(\tau). \quad (3.36)$$

In the following we will discuss the stable dynamic states from the solutions (3.34)–(3.36) for $0 < \lambda < 1$.

(1) When $\theta(0) = \pi/2$, we have $C = \infty$ from (3.33). Hence, $n_2 = 0$, $n_1 = \cos a(\tau)$, $n_3 = \sin a(\tau)$. This shows that the rodlike particles are tumbling in the shear plane since $a(\tau)$ is a strictly decreasing function.

(2) When $\theta(0) = 0$, we have $C = 0$. Hence (3.34)–(3.36) implies $n_2 = 1$, $n_1 = n_3 = 0$. It can be seen that the rodlike particles are always log-rolling around the axial n_2 .

(3) When $\theta(0) \neq 0, \pi/2$, we know from (3.33) that C is bounded. Thus, n_1, n_2 and n_3 are all periodic functions of τ . This implies that the rodlike particles are kayaking. Moreover, the asymmetric axis of the kayaking is also periodic.

Combining the above with the expression (3.12) of λ and Fig. 5 of λ depending on α , we can state the following results.

(i) When $0 < \alpha < \bar{\alpha}$, $\lambda > 1$; flow-aligning (3.30) is the unique stable solution of (3.10). This means that liquid crystal particles are flow-aligning in the shear plane when the intensity α of interaction among particles is weak.

(ii) When $\alpha > \bar{\alpha}$, $0 < \lambda < 1$: the stable dynamic solutions of (3.10) are log-rolling, tumbling and kayaking, depending on the initial states of the liquid crystal particles. It implies that liquid crystal particles are log-rolling, tumbling and kayaking when their initial directions are perpendicular to the shear plane, in the shear plane and other cases, respectively, if the intensity α of the interaction among particles is strong.

4. Conclusion remarks

By rigorous stability analysis we have shown that there is a hysteresis phenomenon for the equilibrium solution of the

Smoluchowski model (1.1) when the flow is at rest. The stable stationary state is from the isotropic phase to the prolate phase when the potential intensity α crosses the critical point 7.5 from small to large, and from the prolate phase to the isotropic phase when α crosses the other critical point 6.731393 from large to small.

From theoretical analysis and numerical calculation we can conclude that log-rolling, flow-aligning, tumbling and kayaking are all stable dynamic states of the liquid crystal particles in a weak shear flow, depending on rod-particles being places. In detail, if the rod-particles are perpendicular to the shear plane, then they are always in the log-rolling state on this vorticity direction. Otherwise, when the intensity α of the interaction among rod particles is weak, the macroscopic flow will determine the directions of the rod-like particles, i.e. rod-particles are in the flow-aligning state for the shear flow when $\alpha \ll 1$. However, when α becomes larger, the rod-particles are in the kayaking or tumbling state. If rod-particles are in the shear plane, they are in the tumbling state. If rod-particles are not in the shear plane, they are kayaking state. Moreover, from numerical calculation we also know that the kayaking state does not circulate around a fixed direction but the vortical axis will change periodically.

Acknowledgments

The authors are very grateful to the referee for his many valuable suggestions and thank Professor Weinan E for his helpful discussions. Hui Zhang is partially supported by an Alexandre von Humboldt Fellowship at Max-Planck Institute for Mathematical Science in Leipzig. Hui Zhang's research is partially supported by the National Science Foundation of China 10401008 and the state key basic research project of China 2005CB321704. Pingwen Zhang's research is partially supported by the state key basic research project of China 2005CB321704 and the National Science Foundation of China for Distinguished Young Scholars 10225103.

References

- [1] L. Archer, R.G. Larson, A molecular theory of flow alignment and tumbling in sheared nematic liquid crystals, *J. Chem. Phys.* 103 (1995) 3108–3111.
- [2] S.G. Baek, J.J. Magda, R.G. Larson, S.D. Hudson, Rheological differences among liquid-crystalline polymers. II. Disappearance of negative N1 in densely packed lyotropes and thermotropes, *J. Rheol.* 38 (1994) 1473–1503.
- [3] G.C. Berry, Bingham Award Lecture C1990: Rheological and rheo-optical studies on nematic solutions of a rodlike polymer, *J. Rheol.* 35 (1991) 943–983.
- [4] A.V. Bhave, R.K. Menon, R.C. Armstrong, R.A. Brown, A constitutive equation for liquid-crystalline polymer solutions, *J. Rheol.* 34 (1993) 413–441.
- [5] D.M. Boudreau, H.H. Winter, C.P. Lillya, R.S. Stein, Conoscopic observations of shear-induced rotations in nematic liquid crystals, *Rheol. Acta* 38 (1999) 503–513.
- [6] W.R. Burghardt, Molecular orientation and rheology in sheared lyotropic liquid crystalline polymers, *Macromol. Chem. Phys.* 199 (1998) 471–488.
- [7] P. Constantin, I. Kevrekidis, E.S. Titi, Asymptotic states of a Smoluchowski equation, *Arch. Ration. Mech. Anal.* 174 (2004) 365–384.

- [8] P. Constantin, I. Kevrekidis, E.S. Titi, Remarks on a Smoluchowski equation, *Discrete Contin. Dyn. Syst.* 11 (2004) 101–112.
- [9] P. Constantin, J. Vukadinovic, Note on the number of steady states for a 2D Smoluchowski equation, *Nonlinearity* 18 (2005) 441–443.
- [10] M. Doi, S.F. Edwards, *The Theory of Polymer Dynamics*, Oxford University Press, 1986.
- [11] W.N. E, P.W. Zhang, Ericksen–Leslie equation derived from a molecular kinetic equation under small Deborah number, Preprint.
- [12] V. Faraoni, M. Grosso, S. Crescitelli, P.L. Maffettone, The rigid-rod model for nematic polymers: An analysis of the shear flow problem, *J. Rheol.* 43 (1999) 829–843.
- [13] I. Fathullin, V. Slastikov, A note on the Onsager model of nematic phase transitions, *Commun. Math. Sci.* 3 (2005) 21–26.
- [14] I. Fathullin, V. Slastikov, Critical points of the Onsager functional on a sphere, *Nonlinearity* 18 (2005) 2565–2580.
- [15] M.G. Forest, Q. Wang, The rigid-rod model for nematic polymers: An analysis of the shear flow problem, *Rheol. Acta* 42 (2003) 20–46.
- [16] M.G. Forest, Q. Wang, R. Zhou, The weak shear kinetic phase diagram for nematic polymers, *Rheol. Acta* 43 (2004) 17–37.
- [17] M.G. Forest, R. Zhou, Q. Wang, Full-tensor alignment criteria for sheared nematic polymers, *J. Rheol.* 47 (2003) 105–127.
- [18] P.G. de Gennes, J. Prost, *The Physics of Liquid Crystals*, 2nd ed., Oxford Science Publications, 1993.
- [19] Ch. Gähwiller, Temperature dependence of flow alignment in nematic liquid crystals, *Phys. Rev. Lett.* 28 (1972) 1554–1556.
- [20] R. Jordan, D. Kinderlehrer, F. Otto, The variational formulation of the Fokker–Planck equation, *SIAM J. Math. Anal.* 29 (1998) 1–17.
- [21] N. Kuzuu, M. Doi, Constitutive equation for nematic liquid crystals under weak velocity gradient derived from a molecular kinetic equation, *J. Phys. Soc. Japan* 52 (1983) 3486–3494.
- [22] R.G. Larson, D.W. Mead, Time and shear-rate scaling laws for liquid crystal polymers, *J. Rheol.* 33 (1989) 1251–1281.
- [23] R.G. Larson, H.C. Öttinger, Effect of molecular elasticity on out-of-plane orientations in shearing flows of liquid-crystalline polymers, *Macromolecules* 24 (1991) 6270–6282.
- [24] H.L. Liu, H. Zhang, P.W. Zhang, Axial symmetry and classification of stationary solutions of Doi–Onsager equation on the sphere with Maier–Saupe potential, *Commun. Math. Sci.* 3 (2005) 201–218.
- [25] C. Luo, H. Zhang, P.W. Zhang, The structure of equilibrium solutions of the one-dimensional Doi equation, *Nonlinearity* 18 (2005) 379–389.
- [26] P.L. Maffettone, S. Crescitelli, Bifurcation analysis of a molecular model for nematic polymers in shear flows, *J. Non-Newtonian Fluid Mech.* 59 (1995) 73–91.
- [27] G. Marrucci, P.L. Maffettone, Description of the liquid crystalline phase of rodlike polymers at high shear rates, *Macromolecules* 22 (1989) 4076–4082.
- [28] L. Onsager, The effects of shape on the interaction of colloidal particles, *Ann. N. Y. Acad. Sci.* 51 (1949) 627–659.
- [29] H. Zhou, H. Wang, M.G. Forest, Q. Wang, A new proof on uniaxial equilibria of Smoluchowski equation for rodlike nematic polymers, *Nonlinearity* 18 (2005) 2815–2825.
- [30] H. Zhou, H.Y. Wang, Steady states and dynamics of 2-D nematic polymers driven by an imposed weak shear, *Commun. Math. Sci.* 5 (2007) 113–132.